Macrocyclic Heterodinuclear $Zn^{II}Pb^{II}$ Complexes: Synthesis, Structures, and Hydrolytic Function toward Tris(*p*-nitrophenyl) Phosphate

Masako Yamami, Hideki Furutachi, Takushi Yokoyama, and Hisashi Ōkawa*

Department of Chemistry, Faculty of Science, Kyushu University, Hakozaki 6-10-1, Higashiku, Fukuoka 812-8581, Japan

Received April 29, 1998

A heterodinuclear $Zn^{II}Pb^{II}$ complex $ZnPb(L)(ClO_4)_2 \cdot 2H_2O$ (**1**) has been obtained where $(L)^{2-}$ is an unsymmetric macrocycle derived from the 2:1:1 condensation of 2,6-diformyl-4-methylphenol, ethylenediamine and diethylenetriamine and has the "salen"- and "saldien"-like metal-binding sites sharing the phenolic moiety. Its DMF adduct, $ZnPb(L)(ClO_4)_2 \cdot MeOH \cdot 2DMF$ (**1′**), crystallizes in the triclinic space group $P\bar{1}$ with $a = 14.457(4)$ Å, $b = 14.795(6)$ Å, $c = 10.307(9)$ Å, $\alpha = 109.04(5)°$, $\beta = 96.24(5)°$, $\gamma = 102.56(3)°$, $V = 1995(2)$ Å^3, and $Z = 2$. The refinement converges with $R = 0.058$ and $R_w = 0.060$ for 3532 reflections with $|F_0| > 3\sigma(|F_0|)$. It has a discrete heterodinuclear core with the Zn^{II} in the "salen" site and the Pb^{II} in the "saldien" site of the macrocycle $(L)^{2-}$. The Zn has a square-pyramidal geometry together with a methanol oxygen, and the Pb has a seven-coordinate geometry together with one DMF oxygen and one perchlorate oxygen. The complex **1** is converted into $[ZnPb(L)(OH)ClO_4]H_2O$ (**2**) under a weak alkaline condition. Its anhydrous form, $[ZnPb(L)(OH)]ClO_4$ (**2**), crystallizes in the monoclinic space group $C2/c$ with $a = 25.835(4)$ Å, $b = 13.190(6)$ Å, $c = 16.553$ Å, $\beta = 106.31(2)°$, $V = 5413(2)$ Å^3, and $Z = 8$. The refinement converges with $R = 0.038$ and $R_w = 0.029$ for 3944 reflections with $|F_0| > 3\sigma(|F_0|)$. It has a dimer structure of a dinuclear $\{ZnPb(L)(OH)\}^+$ unit having the Zn^{II} in the "salen" site and the Pb^{II} in the "saldien" site of the macrocycle. The hydroxide is bound to the Zn^{II} to afford a square-pyramidal geometry about the metal. The dimeric core $[ZnPb(L)(OH)]_2^{2+}$ is formed by the bridge of the hydroxide oxygen to the Pb* of the adjacent molecule and vice versa. The geometry about the Pb in the dimer structure is a pentagonal pyramid showing a distortion to "umbrella-like" structure, with the bridging hydroxide oxygen at the apex. In a DMSO solution, an equilibrium exists between the dimeric and monomeric species: $[\{ZnPb(L)(OH)\}_2]^{2+} \rightleftharpoons 2[ZnPb(L)(OH)]^+$. On the basis of ^{31}P NMR and visible spectra, **2** is shown to hydrolyze tris(*p*-nitorophenyl) phosphate (TNP) into bis(*p*-nitrophenyl) phosphate (BNP) in DMSO. **1** also exhibits a low activity to hydrolyze TNP into BNP due to the equilibrium $[ZnPb(L)(H_2O)]^{2+} \rightleftharpoons [ZnPb(L)(OH)]^+ + H^+$. From the reaction mixture with **2**, a BNP complex $[ZnPb(L)(BNP)]ClO_4$ (**3**) has been isolated. **3** crystallizes in the triclinic space group $P\bar{1}$ with $a = 13.494(9)$ Å, $b = 13.88(1)$ Å, $c = 12.765(8)$ Å, $\alpha = 94.71(6)°$, $\beta = 97.02(6)°$, $\gamma = 61.68(5)°$, $V = 2088(2)$ Å^3, $Z = 2$. The refinement converges with $R = 0.044$ and $R_w = 0.056$ for 6070 reflections with $|F_0| > 3\sigma(|F_0|)$. The BNP^- group bridges the pair of metal ions through its two oxygens, together with two phenolic oxygens of $(L)^{2-}$. On the basis of the above findings, a mechanistic scheme for the TNP hydrolysis by **2** is proposed; a TNP molecule is bound to the Pb center, and the hydroxide on the adjacent Zn ion attacks the phosphorus nucleus of TNP, leading to the formation of the BNP complex **3**.

Introduction

Bimetallic cores exist at the active sites of many metalloenzymes and play essential roles in biological systems by the interplay of a pair of metal ions.[1] A typical example is phosphatases that require at least two metal ions (Mg, Zn, Fe, or Mn) in close proximity to hydrolyze phosphate esters.[1−6] Recent X-ray structural studies for phospholipase C from *Bacillus cereus*,[7] phosphotriesterase from *Pseudomonas diminuta*,[8] and alkaline phosphatase from *E. coli*[9] have revealed that the dinuclear zinc core in these enzymes is unsymmetric with respect to the geometric environments of the two metal ions. It is thought that these phosphatases employ an unsymmetrical dinuclear core to facilitate the concerted binding of the substrate on one metal center and the nucleophilic attack of water or hydroxide at the other metal center.[10] Some model studies have been carried out to mimic the phosphatase function using simple dinuclear metal complexes,[11] and these studies have clarified the significance of two closely held metal centers in phosphate ester hydrolysis.

Recently, heterobimetallic cores were recognized at the active sites of purple acid phosphatase (FeZn),[12] human calcineurin (FeZn),[13] and human protein phosphatase 1 (MnFe),[14] and these

(1) (a) Fenton, D. E.; Ōkawa, H. *Perspectives on Bioinorganic Chemistry*; JAI Press: London, 1993; Vol. 2, p 81. (b) Karlin, K. D. *Science* **1993**, *261*, 701.
(2) Wilcox, D. E. *Chem. Rev.* **1996**, *96*, 243.
(3) Lipscomb, W. N.; Sträter, N. *Chem. Rev.* **1996**, *96*, 2357.
(4) Dismukes, G. C. *Chem. Rev.* **1996**, *96*, 2909.
(5) Sträter, N.; Lipscomb, W. N.; Klabunde, T.; Krebs, B. *Angew. Chem., Int. Ed. Engl.* **1996**, *35*, 2024.
(6) Steinhagen, H.; Helmchem, G. *Angew. Chem., Int. Ed. Engl.* **1996**, *35*, 2339.
(7) Hough, E.; Hansen, L. K.; Birknes, B.; Jynge, K.; Hansen, S.; Hordvik, A.; Little, C.; Dodson, E. J.; Derewenda, Z. *Nature (London)* **1989**, *338*, 357.
(8) Vanhooke, J. L.; Benning, M. M.; Raushel, F. M.; Holden, H. M. *Biochemistry* **1996**, *35*, 6020.
(9) Kim, E. E.; Wyckoff, H. W. *J. Mol. Biol.* **1991**, *218*, 449.
(10) Kimura, E. *Prog. Inorg. Chem.* **1994**, *41*, 443.

10.1021/ic9804869 CCC: $15.00
Published on Web 12/04/1998

Chart 1. Chemical Structure of $(L)^{2-}$

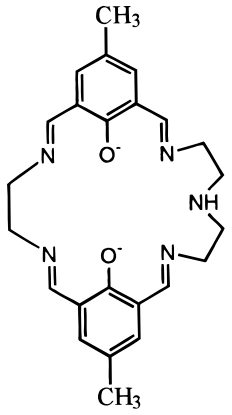

findings have stimulated interest in the cooperative function of a pair of dissimilar metal ions in phosphate ester hydrolysis. The heterobimetallic cores of these enzymes can be considered as metamorphic forms of the unsymmetric homobimetallic cores previously discussed. Heterodinuclear complexes bridged by a phosphate monoester dianion or a phosphate diester anion were reported.[15,16] This study aims to provide a functional model of heterobimetallic phosphatases to demonstrate the interplay of a pair of dissimilar metal ions in phosphate ester hydrolysis.

The essential step for the model study is to prepare a discrete and stable heterodinuclear core complex of an appropriate pair of dissimilar metal ions in close proximity. For this purpose, the use of a compartmental ligand whose two metal-binding sites are not equivalent is recommended. The phenol-based macrocycle $(L)^{2-}$ (Chart 1), having "salen"- and "saldien"-like metal-binding sites sharing the phenolic moiety, was developed in this laboratory[17−21] (salen = *N*,*N*′-ethylenedisalicylideneaminate; saldien = *N*,*N*′-1,5-(3-azapentylene)disalicylideneaminate). It forms a series of heterodinuclear $M_a^{II}M_b^{II}$ (M_a = Cu, Ni, Co; M_b = Pb, Mn, Fe, Co, Ni, Cu, Zn) complexes having the M_a^{II} ion at the "salen"-like N_2O_2 site and the M_b^{II} ion at the "saldien"-like N_3O_2 site.

In this study, this ligand is adopted to prepare $Zn^{II}Pb^{II}$ complexes for modeling heterobimetallic phosphatases. The metal ion pair is chosen by taking into consideration the nature of Zn^{II} to form $Zn^{II}-OH$ linkages and the high affinity of Pb^{II} toward phosphate oxygen. A ZnPb complex $ZnPb(L)(ClO_4)_2\cdot 2H_2O$ (**1**) is derived from the ligand, and **1** is converted into a hydroxo complex, $[ZnPb(L)(OH)]ClO_4$ (**2**), under a weak alkaline condition. The main focus is placed on a phosphatase-like function of **2** to hydrolyze tris(*p*-nitrophenyl) phosphate (TNP) to bis(*p*-nitrophenyl) phosphate (BNP). A part of this work was preliminarily reported.[22]

Experimental Section

Physical Measurements. Elemental analyses of C, H, and N were obtained at the Elemental Analysis Service Center of Kyushu University. Analyses of Zn were obtained using a Shimadzu AA-660 atomic absorption/flame emission spectrometer. Infrared spectra were recorded on a JASCO IR-810 spectrometer using KBr disks or Nujol mulls. Electronic spectra were recorded using a Shimadzu UV-3100PC spectrometer. ^{1}H NMR and ^{13}C NMR spectra (400 MHz) were recorded on a JEOL JNM-GX 400 using tetramethylsilane as the internal standard. ^{31}P NMR spectra (400 MHz) were recorded on a JEOL JNM-GX 400 spectrometer using H_3PO_4 (85%) as the external reference. Positive ion fast atom bombardment (FAB) mass spectra were recorded on a JEOL JMS-SX 102A BE/BE four-sector-type tandem mass spectrometer using *m*-nitrobenzyl alcohol as the matrix.

Preparation. 2,6-Diformyl-4-methylphenol was prepared by the method of Denton and Suschitzky.[23] *N*,*N*′-Bis(3-formyl-5-methylsalicylidene)ethylenediamine,[24] *N*,*N*′-bis(3-formyl-5-methylsalicylidene)-ethylenediaminatonickel(II),[24] $[NiPb(L)](ClO_4)_2\cdot H_2O$,[18] and $[Zn(salen)(H_2O)]$[25] were prepared by the literature methods. Other chemicals were of reagent grade and used as purchased. **Caution:** the perchlorate complexes described below may be explosive and should be prepared in small portions.

***N*,*N*′-Bis(3-formyl-5-methylsalicylidene)ethylenediaminatozinc-(II).** To a suspension of *N*,*N*′-bis(3-formyl-5-methylsalicylidene)-ethylenediamine (2.0 g, 5.7 mmol) in methanol (20 cm^3) was added a methanol solution of $Zn(CH_3COO)_2\cdot 2H_2O$ (1.25 g, 5.7 mmol), and the mixture was refluxed for 1 h to form a yellow powder. It was used for the preparation of the following complexes without further purification. The yield was 1.5 g (63%). Selected IR data (ν/cm^{-1} using KBr): 2900, 1640.

$ZnPb(L)(ClO_4)_2\cdot 2H_2O$ (1). A suspension of *N*,*N*′-bis(3-formyl-5-methylsalicylidene)ethylenediaminatozinc(II) (1.66 g, 4 mmol) in methanol (30 cm^3) and a solution of lead(II) perchlorate trihydrate (1.8 g, 4 mmol) in methanol (30 cm^3) were mixed and stirred at ambient temperature for 30 min. A methanol solution (10 cm^3) of diethylenetriamine (0.41 g, 4 mmol) was added dropwise, and the mixture was refluxed for 1 h to give a yellow powder. It was collected by suction filtration, washed successively with 2-propanol and ether, and dried in vacuo. The yield was 2.96 g (80%). Anal. Found: C, 30.97; H, 3.16; N, 7.91; Zn, 6.7%. Calcd for $C_{24}H_{31}N_5O_{12}Cl_2PbZn$: C, 31.16; H, 3.38; N, 7.57; Zn, 7.1%. FAB mass [*m*/*z*]: 788 for $\{ZnPb(L)(ClO_4)\}^+$. Selected IR data [ν/cm^{-1}] using KBr: 3300, 2900, 2850, 1650, 1100. ^{1}H NMR [δ/ppm] in DMSO-d_6: 8.606 (s, 2H, −CH═N−(en)−N═HC−), 8.531 (s, 2H, −CH═N−(dien)−N═HC−), 7.417 (s, 2H, ring),

(11) (a) Seo, J. S.; Sung, N.; Hynes, R. C.; Chin, J. *Inorg. Chem.* **1996**, *35*, 7472. (b) Vance, D. H.; Czarnik, A. W. *J. Am. Chem. Soc.* **1993**, *115*, 12165. (c) Chapman, W. H., Jr.; Breslow, R. *J. Am. Chem. Soc.* **1995**, *117*, 5462. (d) Yashiro, M.; Ishikubo, A.; Komiyama, M. *J. Chem. Soc., Chem. Commun.* **1995**, 1793. Irisawa, M.; Takeda, N.; Komiyama, M. *J. Chem. Soc., Chem. Commun.* **1995**, 1221. (e) Koike, T.; Inoie, M.; Kimua, E.; Shiro, M. *J. Am. Chem. Soc.* **1996**, *118*, 3091. (f) Hurst, P.; Takasaki, B. K.; Chin, J. *J. Am. Chem. Soc.* **1996**, *118*, 9982. (g) Tsuboushi, A.; Bruice, T. C. *J. Am. Chem. Soc.* **1994**, *116*, 11614. (h) Ragunathan, K. G.; Schneider, H. J. *Angew. Chem., Int. Ed. Engl.* **1996**, *35*, 1219. (i) Molenveld, P.; Kapsabeils, S.; Engbersen, J. F. J.; Reinhoudt, D. N. *J. Am. Chem. Soc.* **1997**, *119*, 2948. (j) Frey, S. T.; Murthy, N. N.; Weintraub, S. T.; Thompson, L. K.; Karlin, K. D. *Inorg. Chem.* **1997**, *36*, 956. (k) Hendry, P.; Sageson, A. M. *Prog. Inorg. Chem.* **1990**, *38*, 201. (l) Hikichi, S.; Tanaka, M.; Morooka, Y.; Kitajima, N. *J. Chem. Soc., Chem. Commun.* **1992**, 814. (m) Bazzicalupi, C.; Bencini, A.; Bianchi, A.; Fusi, V.; Giorgi, C.; Paoletti, P.; Valtancoli, B.; Zanchi, D. *Inorg. Chem.* **1997**, *36*, 2784.

(12) Strater, N.; Klabunde, T.; Tucker, P.; Witzel, H.; Krebs, B. *Science* **1995**, *268*, 1489.

(13) Kissinger, C. R.; Parge, H. E.; Knighton, D. R.; Lewis, C. T.; Pelletier, L. A.; Tempczyk, A.; Kalish, V. J.; Tucker, K. D.; Showalter, R. E.; Moomaw, E. W.; Gastinel, L. N.; Habuka, N.; Chen, X.; Maldonado, F.; Barker, J. E.; Bacquet, R.; Villafranca, E. *Nature* **1995**, *378*, 641.

(14) Engloff, M.-P.; Cohen, P. T. W.; Reinemer, P.; Barford, D. *J. Mol. Biol.* **1995**, *254*, 942.

(15) Schepers, K.; Bremer, B.; Krebs, B.; Henkel, G.; Althaus, E.; Mosel, B.; Müller-Warmuth, W. *Angew. Chem., Int. Ed. Engl.* **1990**, *29*, 531.

(16) Tanase, T.; Yun, J. W.; Lippard, S. J. *Inorg. Chem.* **1996**, *35*, 3585 and references therein.

(17) Ōkawa, H.; Nishio, J.; Ohba, M.; Tadokoro, M.; Matsumoto, N.; Koikawa, M.; Kida, S.; Fenton, D. E. *Inorg. Chem.* **1993**, *32*, 2949.

(18) Nishio, J.; Ōkawa, H.; Ohtsuka, S.; Tomono, M. *Inorg. Chim. Acta* **1994**, *218*, 27.

(19) Shimoda, J.; Furutachi, H.; Yonemura, M.; Ohba, M.; Matsumoto, N,; Ōkawa, H. *Chem Lett.* **1996**, 979.

(20) Furutachi, H.; Ōkawa, H. *Inorg. Chem.* **1997**, *36*, 3911.

(21) Furutachi, H.; Ōkawa, H. *Bull. Chem. Soc. Jpn.* **1998**, *71*, 671.

(22) Yamami, M.; Furutachi, H.; Yokoyama, T.; Ōkawa, H. *Chem. Lett.* **1988**, 211.

(23) Denton, D. A.; Suschitzky, H. *J. Chem. Soc.* **1963**, 4741.

(24) (a) Ōkawa, H.; Kida, S. *Inorg. Nucl. Chem. Lett.* **1971**, *7*, 751. (b) Ōkawa, H.; Kida, S. *Bull. Chem. Soc. Jpn.* **1972**, *45*, 1759.

(25) Hall, D.; Moore, F. H. *J. Chem. Soc.* **1966**, 1822.

Table 1. Summary of Crystal Data for Complexes **1′**, **2′**, and **3**

complex	**1′**	**2′**	**3**
formula	$C_{31}H_{45}O_{13}N_7Cl_2ZnPb$	$C_{24}H_{28}O_7N_5ClZnPb$	$C_{36}H_{35}O_{14}N_7ClZnPPb$
cryst color	yellow	yellow	yellow
MW	1067.22	806.55	939.06
cryst. dimens (mm)	0.25 × 0.10 × 0.10	0.50 × 0.10 × 0.20	0.25 × 0.15 × 0.15
cryst. syst.	triclinic	monoclinic	triclinic
space group	$P\bar{1}$	$C2/c$	$P\bar{1}$
a (Å)	14.457(4)	25.835(4)	13.494(9)
b (Å)	14.795(6)	13.190(6)	13.88(1)
c (Å)	10.307(9)	16.553(6)	12.765(8)
α (deg)	109.04(5)	90	94.71(6)
β (deg)	96.24(5)	106.31(2)	97.02(6)
γ (deg)	102.56(3)	90	61.68(5)
V (Å^3)	1995(2)	5413(2)	2088(2)
Z	2	8	2
D_c (g cm^{-3})	1.776	1.979	1.795
R^a	0.058	0.038	0.044
$R_w^{b,c}$	0.060	0.029	0.056

[a] $R = \sum||F_o| - |F_c||/\sum|F_o|$. [b] $R_w = \{\sum[w(|F_o| - |F_c|)^2]/\sum[wF_o^2]\}^{1/2}$. [c] $w = 1/\sigma^2(F_o)$.

7.413 (s, 2H, ring), 2.268 (s, 6H, Me). ^{13}C NMR [δ/ppm] in DMSO-d_6: 169.0 and 167.8 (azomethine C); 165.0, 141.9, 140.7, 124.7, 123.4, and 121.4 (ring C); 63.7 (=N*C*H$_2$*C*H$_2$N=); 54.9 (=N*C*H$_2$*C*H$_2$-NHCH$_2$*C*H$_2$N=); 51.5 (=NCH$_2$*C*H$_2$NH*C*H$_2$*C*H$_2$N=); 19.3 (methyl C). UV−vis [λ_{max}/nm (ϵ/M^{-1} cm^{-1})] in DMSO: 266 (30 700), 383 (15 000).

It was crystallized from a 2-propanol/dimethylformamide/methanol mixture (2:1:1 in volume) as ZnPb(L)(ClO$_4$)$_2$·MeOH·2DMF (**1′**) suitable for X-ray crystallography. Anal. Found: C, 34.60; H, 4.04; N, 9.34%. Calcd for $C_{31}H_{45}N_7O_{13}Cl_2ZnPb$: C, 34.89; H, 4.25; N, 9.19%.

ZnPb(L)(OH)ClO$_4$·H$_2$O (2). To an acetonitrile solution (20 cm^3) of **1** (0.231 g, 0.25 mmol) was added triethylamine (0.026 g, 0.25 mmol). The mixture was stirred for 30 min to give yellow microcrystals. They were collected by suction filtration, washed successively with 2-propanol and ether, and dried in vacuo. The yield was 0.144 g (70%). Anal. Found: C, 34.95; H, 3.44; N, 8.44; Zn, 7.6%. Calcd for $C_{24}H_{30}N_5O_8ClZnPb$: C, 34.96; H, 3.67; N, 8.49; Zn, 7.9%. FAB mass [*m*/*z*]: 688 for {ZnPb(L)−H}$^+$. Selected IR data [ν/cm^{-1}] using KBr: 3580, 3250, 2900, 2850, 1640, 1100. ^{1}H NMR [δ/ppm] in DMSO-d_6 at 5 × 10^{-2} M: 8.339 (s, 2H, −CH=N−(en)−N=HC−), 7.929 (s, 2H, −CH=N−(dien)−N=HC−), 7.100 (s, 2H, ring), 7.075 (s, 2H, ring), 2.267 (s, 6H, Me). ^{13}C NMR [δ/ppm] in DMSO-d_6: 168.7 and 165.7 (azomethine C); 164.6, 142.1, 140.0, 124.3, 122.1, and 121.5 (ring C); 61.5 (=N*C*H$_2$*C*H$_2$N=); 57.1 (=N*C*H$_2$CH$_2$NHCH$_2$*C*H$_2$N=); 49.1 (=NCH$_2$*C*H$_2$NH*C*H$_2$*C*H$_2$N=); 19.4 (methyl C). UV−vis [λ_{max}/nm (ϵ/M^{-1} cm^{-1})] in DMSO: 266 (31 100), 378 (14 400).

Recrystallization from a 2-propanol/acetonitrile mixture (1:1 in volume) formed [ZnPb(OH)]ClO$_4$ (**2′**) suitable for X-ray crystallography. Anal. Found: C, 35.82; H, 3.62; N, 8.65%. Calcd for $C_{24}H_{28}N_5O_7ClZnPb$: C, 3.50; H, 35.74; N, 8.68%.

[ZnPb(L)(BNP)]ClO$_4$ (3). a. Method 1. To a solution of **2** (0.083 g, 0.1 mmol) in acetonitrile (30 cm^3) was added tris(*p*-nitrophenyl) phosphate (0.046 g, 0.1 mmol), and the mixture was stirred for 1 h at room temperature. The resulting yellow solution was once filtered to separate any insoluble material and allowed to stand for 2 days to form yellow microcrystals. They were collected by suction filtration and dried in vacuo. The yield was 56%. Anal. Found: C, 38.57; H, 3.24; N, 8.71; Zn, 6.1%. Calcd for $C_{36}H_{35}N_7O_{14}ClPZnPb$: C, 38.31; H, 3.13; N, 8.69; Zn, 5.8%. FAB mass [*m*/*z*]: 1028 for {ZnPb(L)(BNP)}$^+$. Selected IR data [ν/cm^{-1}] using KBr: 3250, 3100, 3050, 2900, 2850, 1650, 1520, 1340, 1210, 1080. ^{1}H NMR [δ/ppm] in DMSO-d_6: 8.554 (s, 2H, −CH=N−(en)−N=HC−), 8.455 (s, 2H, −CH=N−(dien)−N=HC−), 8.209 (d, J = 9 Hz, 4H, ring), 7.347 (d, J = 9 Hz, 4H, ring), 7.260 (s, 2H, ring), 7.240 (s, 2H, ring), 2.249 (s, 6H, Me). ^{13}C NMR [δ/ppm] in DMSO-d_6: 168.8 and 167.0 (azomethine C); 164.8, 142.0, 140.7, 124.5, 122.9, and 121.2 (ring C of the macrocycle); 157.9, 142.3, 125.1, and 120.1 (ring C of BNP$^-$); 63.0 (=N*C*H$_2$*C*H$_2$N=); 55.1 (=N*C*H$_2$CH$_2$NHCH$_2$*C*H$_2$N=); 50.6 (=NCH$_2$CH$_2$NHCH$_2$CH$_2$N=); 19.1 (methyl C). UV−vis [λ_{max}/nm (ϵ/M^{-1} cm^{-1})] in DMSO: 270 (30 800), 376 (12 400).

b. Method 2. A portion of **1** (0.093 g, 0.1 mmol) was dissolved in acetonitrile (10 cm^3), and this solution was mixed with an acetonitrile solution containing tris(*p*-nitrophenyl) phosphate (0.046 g, 0.1 mmol). The mixture was stirred at room temperature for 30 min. The addition of triethylamine (0.010 g, 0.1 mmol) followed by further stirring at room temperature resulted in the precipitation of yellow microcrystals. The yield was 53%.

Crystal Structure Analyses. Each single crystal of **1′** and **3** was mounted on a glass fiber and coated with epoxy resin. A single crystal of **2′** was sealed in a glass tube. Intensities and lattice parameters were obtained on a Rigaku AFC-7R automated four-circle diffractometer, using graphite-monochromated MoKα radiation (λ = 0.71069 Å) and a 12 kW rotating anode generator at 231 °C. The cell parameters were determined by 25 reflections in the 2θ range of 28.82° < 2θ < 29.98° for **1′**, 29.70° < 2θ < 29.98° for **2′**, and 29.83° < 2θ < 30.04° for **3**. For the intensity data collections, the ω−2θ scan mode was used to a maximum 2θ value of 45.1° for **1′**, 55.0° for **2′**, and 50.0° for **3** at the scan rate of 16° min^{-1}. The weak reflections (I < 10.0σ(I)) were rescanned (maximum of 4 scans), and the counts were accumulated to ensure good counting statistics. Stationary background counts were recorded on each side of the reflection. The ratio of peak counting time to background counting time was 2:1. The diameter of the incident beam collimator was 1.0 mm, the crystal-to-detector distance was 235 mm, and the computer-controlled detector aperture was set to 9.0 mm × 13.0 mm (horizontal × vertical). Three standard reflections were monitored every 150 reflections. Over the course of the data collection, the standards decreased by 13.84% for **1′**, 7.0% for **2′**, 1.8% for **3**. A linear correction factor was applied to the data to account for the phenomena. The linear absorption coefficient, μ, for MoKα radiation was 50.26 cm^{-1} for **1′**, 72.60 cm^{-1} for **2′**, and 47.8 cm^{-1} for **3**. An empirical absorption correction based on azimuthal scans of several reflections was applied, which resulted in transmission factors ranging from 0.79 to 1.00 for **1′**, from 0.75 to 1.00 for **2′**, and from 0.81 to 1.00 for **3**. The intensity data were corrected for Lorentz and polarization factors. Pertinent crystallographic parameters for **1′**, **2′**, and **3** are given in Table 1.

The structures were solved by direct methods and expanded using Fourier techniques. Refinements were carried out by the full-matrix least-squares method, where the function minimized is $\sum w(|F_o| - |F_c|)^2$ with $w = 1/\sigma^2(F_0)$. Non-hydrogen atoms were refined anisotropically. Hydrogen atoms were fixed at the calculated positions and were not refined.

Neutral atom scattering factors were taken from Cromer and Waber.[26] Anomalous dispersion effects were included in F_{calc}; the values for $\Delta f'$ and $\Delta f''$ were those of Creagh and McAuley.[27] The values for the mass attenuation coefficients were those of Creagh and Hubbel.[28] All

(26) Cromer, D. T.; Waber, J. T. *International Tables for X-ray Crystallography*; Kynoch Press: Birmingham, 1974; Vol. IV.

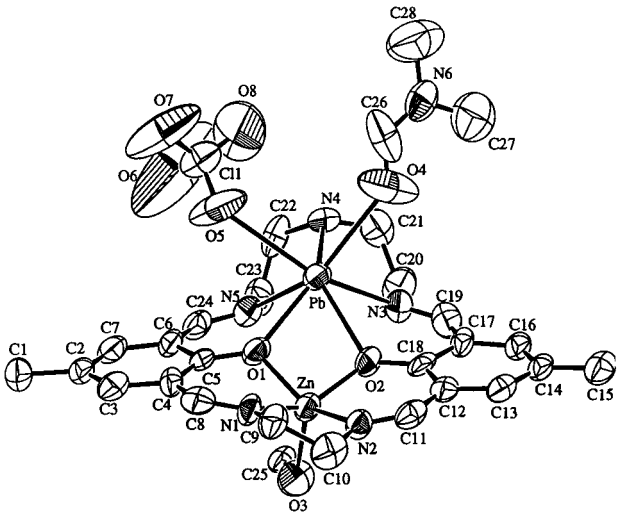

Figure 1. ORTEP view of the cation of **1′** with the atom numbering scheme.

calculations were performed using the TEXSAN crystallographic software package of Molecular Structure Corporation.[29]

Results and Discussions

Synthesis of ZnPb Complexes. In our previous studies, the macrocyclic ligand $(L)^{2-}$ was prepared as $M^{II}Pb^{II}$ complexes (M = Cu, Ni, or Co) by the stepwise template reaction that uses two metal ions, M^{II} and Pb^{II}, at different stages in the cyclization.[17−21] That is, an acyclic ligand complex, *N*,*N*′-bis-(3-formyl-5-methylsalicylidene)ethylenediaminatometal(II), was prepared that was then reacted with diethylenetriamine in the presence of the Pb^{II} ion. In this study, this method was successfully applied for preparing $ZnPb(L)(ClO_4)_2 \cdot 2H_2O$ (**1**). It contains two water molecules, of which one water must be coordinated to the Zn center as judged from the five-coordinate geometry of $[Zn(salen)(H_2O)]$.[25]

Complex **1** was converted into $[ZnPb(L)(OH)]ClO_4 \cdot H_2O$ (**2**) when triethylamine was added to an acetonitrile solution of **1**. This fact means that one of the water molecules is acidic enough to be deprotonated under weak alkaline conditions. The pK_a value for the bound water could not be determined in this work because **1** is insoluble in water and alcohols. The use of aqueous sodium hydroxide instead of triethylamine gave unsatisfactory results because of the elimination of Zn^{II} as $Zn(OH)_2$.

Crystal Structures. **a. $ZnPb(L)(ClO_4)_2 \cdot MeOH \cdot 2DMF$ (1′).** An ORTEP[30] view of the cation of **1′** is shown in Figure 1 together with the numbering scheme. Selected bond distances and angles are given in Table 2.

The essential part of **1′** consists of the macrocycle $(L)^{2-}$, Zn^{II} and Pb^{II} ions, a methanol molecule, a DMF molecule, and a perchlorate ion. One DMF molecule and one perchlorate ion are free from coordination and located in the lattice. The Zn^{II} and Pb^{II} ions are bridged by the phenolic oxygens, O1 and O2, with an intermetallic separation of 3.653(2) Å.

The Zn resides in the "salen" site of the macrocycle $(L)^{2-}$ and assumes a square-pyramidal geometry together with the methanol oxygen O3 at the axial site. The displacement of the Zn from the basal least-squares plane toward the methanol oxygen O3 (0.60 Å) is fairly large relative to the displacement of the metal in the analogous CuPb and CoPb complexes.[17,19] The basal Zn−N and Zn−O bond distances fall in the range 2.01(1)−2.08(1) Å, which are longer than the corresponding bond distances of the CuPb and CoPb complexes, in accord with the large displacement of the Zn in **1′**. The axial Zn−O3 bond distance (2.09(1) Å) is slightly longer than the basal bond distances.

Table 2. Relevant Bond Distances and Angles for **1′**

Bond Distances (Å)			
Zn−O(1)	2.01(1)	Pb−O(1)	2.52(1)
Zn−O(2)	2.01(1)	Pb−O(2)	2.60(1)
Zn−O(3)	2.09(1)	Pb−O(4)	2.77(2)
Zn−N(1)	2.08(1)	Pb−O(5)	2.99(2)
Zn−N(2)	2.05(1)	Pb−N(3)	2.50(1)
		Pb−N(4)	2.59(2)
		Pb−N(5)	2.48(1)
Bond Angles (deg)			
O(1)−Zn−O(2)	84.8(4)	O(1)−Pb−O(2)	63.9(3)
O(1)−Zn−O(3)	101.3(5)	O(1)−Pb−O(4)	146.3(5)
O(1)−Zn−N(1)	85.7(5)	O(1)−Pb−O(5)	79.8(4)
O(1)−Zn−N(2)	146.6(5)	O(1)−Pb−N(3)	118.9(4)
O(2)−Zn−O(3)	106.9(5)	O(1)−Pb−N(4)	138.3(4)
O(2)−Zn−N(1)	144.2(5)	O(1)−Pb−N(5)	68.8(4)
O(2)−Zn−N(2)	89.0(5)	O(2)−Pb−O(4)	104.0(5)
O(3)−Zn−N(1)	108.8(5)	O(2)−Pb−O(5)	135.0(4)
O(3)−Zn−N(2)	111.9(5)	O(2)−Pb−N(3)	68.3(4)
N(1)−Zn−N(2)	80.4(6)	O(2)−Pb−N(4)	136.2(4)
Pb−O(1)−Zn	106.7(5)	O(2)−Pb−N(5)	109.3(4)
Pb−O(2)−Zn	104.2(4)	O(4)−Pb−O(5)	91.5(6)
		O(4)−Pb−N(3)	79.9(6)
		O(4)−Pb−N(4)	73.0(5)
		O(4)−Pb−N(5)	141.5(5)
		O(5)−Pb−N(3)	156.7(5)
		O(5)−Pb−N(4)	88.6(5)
		O(5)−Pb−N(5)	78.5(5)
		N(3)−Pb−N(4)	68.2(4)
		N(3)−Pb−N(5)	94.7(5)
		N(4)−Pb−N(5)	69.7(5)

The Pb in the "saldien" site has a seven-coordinate geometry together with one DMF oxygen O4 and one perchlorate oxygen O5. The Pb deviates by 1.31 Å from the least-squares plane defined by N3, N5, O1, and O2. The two exogenous donor atoms occupying the open space of the Pb^{II} (the DMF oxygen O4 and the perchlorate oxygen O5) are situated trans to the methanol oxygen O3 bound to Zn(II), with respect to the mean molecular plane. The Pb−O4 (2.77(2) Å) and Pb−O5 (2.99(2) Å) bond distances are longer than the Pb−L bond distances (2.48(1)−2.60(1) Å).

b. $[ZnPb(L)(OH)]ClO_4$ (2′). The crystal has a dimer structure of the dinuclear $\{ZnPb(L)(OH)\}^+$ unit; the perchlorate ion is free from coordination and captured in the lattice. An ORTEP view of the $\{ZnPb(L)(OH)\}^+$ unit with the atom numbering scheme is shown in Figure 2 and that of the dimer structure is given in Figure 3. Selected bond distances and angles are listed in Table 3.

The Zn^{II} and Pb^{II} ions are bridged by the endogenous phenolic oxygens, O1 and O2, with an intermetallic Zn−Pb separation of 3.522(1) Å. The Zn resides in the "salen" site of the macrocycle and assumes a square-pyramidal geometry together with the hydroxide oxygen O3 at the apex. The dimeric core $[ZnPb(L)(OH)]_2^{2+}$ is formed by the bridge of the hydroxo oxygen O3 to the Pb* of the adjacent molecule and the bridge of O3* to Pb. The basal Zn-to-macrocycle bond distances fall in the range 2.022(5)−2.088(7) Å. The axial Zn−O3 bond

(27) Creagh, D. C.; McAuley, W. J. *International Tables for X-ray Crystallography*; Wilson, A. J. C., et al., Eds.; Kluwer Academic Publishers: Boston, 1992; pp 219−222.
(28) Creagh, D. C.; Hubbell, J. H. *International Tables for X-ray Crystallography*; Wilson, A. J. C., et al., Eds.; Kluwer Academic Publishers: Boston, 1992; pp 200−206.
(29) *TEXSAN*; Molecular Structure Corporation: Houston, TX, 1985.
(30) Johnson, C. K. Report 3794; Oak Ridge National Laboratory: Oak Ridge, TN, 1965.

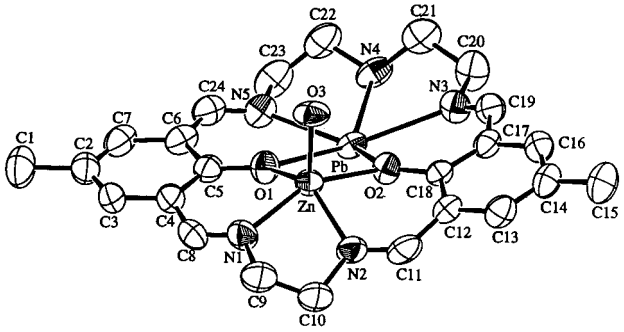

Figure 2. ORTEP view of the $\{ZnPb(L)(OH)\}^{+}$ unit of **2′** with the atom numbering scheme.

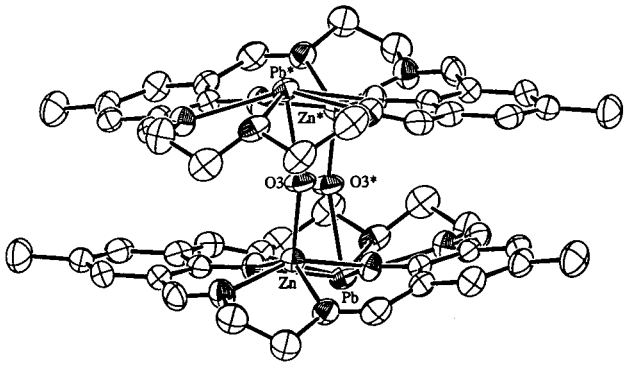

Figure 3. Depiction of the dimer structure of **2′**.

Table 3. Relevant Bond Distances and Angles for **2′**

	Bond Distances (Å)		
Zn−O(1)	2.022(5)	Pb−O(1)	2.636(6)
Zn−O(2)	2.057(5)	Pb−O(2)	2.553(5)
Zn−O(3)	1.918(5)	Pb−O(3)*	2.276(5)
Zn−N(1)	2.083(8)	Pb−N(3)	2.595(8)
Zn−N(2)	2.088(7)	Pb−N(4)	2.551(8)
		Pb−N(5)	2.578(7)
	Bond Angles (deg)		
O(1)−Zn−O(2)	93.7(2)	O(1)−Pb−O(2)	69.9(2)
O(1)−Zn−O(3)	108.6(2)	O(1)−Pb−O(3)*	71.7(2)
O(1)−Zn−N(1)	87.3(3)	O(1)−Pb−N(3)	137.2(2)
O(1)−Zn−N(2)	139.1(3)	O(1)−Pb−N(4)	135.3(2)
O(2)−Zn−O(3)	94.4(2)	O(1)−Pb−N(5)	70.7(2)
O(2)−Zn−N(1)	152.7(3)	O(2)−Pb−O3*	77.7(2)
O(2)−Zn−N(2)	83.7(3)	O(2)−Pb−N(3)	71.6(2)
O(3)−Zn−N(1)	111.2(3)	O(2)−Pb−N(4)	137.3(2)
O(3)−Zn−N(2)	112.3(3)	O(2)−Pb−N(5)	137.8(2)
N(1)−Zn−N(2)	78.0(3)	O(3)*−Pb−N(3)	82.4(2)
Pb−O(1)−Zn	97.4(2)	O(3)*−Pb−N(4)	80.7(2)
Pb−O(2)−Zn	99.1(2)	O(3)*−Pb−N(5)	76.2(2)
Pb−O(3)−Zn	165.0(3)	N(3)−Pb−N(4)	69.3(2)
		N(3)−Pb−N(5)	135.5(2)
		N(4)−Pb−N(5)	69.1(3)

length is short (1.918(5) Å) and compared to the Zn−O bond distances found for μ-hydroxo zinc complexes.[31,32] The displacement of the Zn from the basal N_2O_2 least-squares plane toward O3 is 0.58 Å. The Pb−O3* bond distance is 2.276(5) Å, and the Zn−O3−Pb* bond angle is 165.0(3)°. The Zn- -Pb* separation is 4.158(1) Å.

The Pb at the N_3O_2 site assumes a six-coordinate geometry together with O3* of the bridging OH^{-}. The geometry about the Pb can be depicted as a pentagonal pyramid with O1, O2, N3, N4, and N5 of the "saldien" site on the base and the OH^{-} ion O3* at the axial position. The Pb is deviated by 0.54 Å from the pentagonal least-squares plane toward the open face to afford an "umbrella-like" distortion about the Pb. The sum of the angles O1−Pb−O2, O2−Pb−N3, N3−Pb−N4, N4−Pb−N5, and O1−Pb−N5 is 350.6°; that is smaller than 360°, in accord with the "umbrella-like" distortion. It must be noted that the Pb−O3* bond distance (2.276(5) Å) is significantly shorter than the Pb−L bond distances (2.551(8)−2.636(6) Å).

The diversity in the core structure for the $M^{II}Pb^{II}$ complexes of $(L)^{2-}$ has been recognized in this laboratory.[17,19,21] The rare "umbrella-like" structure about the Pb of **2′** is probably associated with an "active lone-pair"[33] situated trans to the bridging OH^{-}.

General Properties. Selected IR spectral data of **1** and **2** are given in the Experimental Section. The IR spectra of the complexes are similar to each other and show the ν(C═N) vibration at 1640−1650 cm^{-1} and the ν(N−H) vibration of the secondary amine on the lateral chain at 3250−3340 cm^{-1}. **2** shows the ν(O−H) vibration at 3580 cm^{-1}. The high frequency of the band is in harmony with the bridging function of the OH^{-} group in the crystal.[34]

The positive ion FAB mass spectra of the ZnPb complexes exhibit parent peaks corresponding to the respective heterodinuclear ZnPb core; no peak corresponding to homodinuclear ZnZn or PbPb species was observed. The molecular ion peak m/z = 788 for **1** corresponds to $\{ZnPb(L)ClO_4\}^{+}$, and the molecular ion peak of m/z = 688 for **2** corresponds to the momomeric species $\{ZnPb(L)^{2+}-H^{+}\}^{+}$.

The electronic absorption spectra of **1** and **2** in DMSO have two intense absorption bands at 270 and ∼380 nm. Both can be assigned to intraligand transition bands. The absorption at ∼380 nm is typical of the azomethine group.[35,36] No absorption is seen in the visible region in accord with the electronic nature of the Zn^{II} and Pb^{II} ions.

The ^{1}H NMR and ^{13}C NMR spectra of **1** and **2** were measured in DMSO-d_6 at room temperature. The numerical data are given in the Experimental Section. Both complexes show a C_s symmetrical feature with respect to the macrocyclic ligand. The ^{1}H NMR spectrum of **1** has four singlets in the region of 8.61−7.41 ppm that are assigned to the nonequivalent azomethine and ring protons. The ^{13}C NMR spectrum has 12 carbon resonances. The ^{1}H NMR spectrum of **2** at 5×10^{-2} M concentration also shows four singlets due to the azomethine and ring protons in the region of 8.34−7.07 ppm. The upfield shift of these signals relative to those of **1** indicates that **2** exists in the dimer structure (Figure 3). At a lower concentration (5×10^{-3} M), however, the ^{1}H NMR spectrum has eight singlet resonances comprised of four dominant resonances at 8.35, 7.94, 7.11, and 7.08 ppm, compared to those for **2** in the dimer structure, and four weaker resonances at 8.31, 7.83, 7.35, and 7.27 ppm. At a lower concentration (1×10^{-3} M), the last four resonances are dominant and the former resonances due to the dimer structure practically disappear. Evidently, **2** exists in an equilibrium between the dimeric and monomeric forms at a lower concentration in DMSO i.e., $[\{ZnPb(L)(OH)\}_2]^{2+} \rightleftharpoons 2[ZnPb(L)(OH)]^{+}$.

(31) Gorrell, I. B.; Looney, A.; Parkin, G. *J. Am. Chem. Soc.* **1990**, *112*, 4068.
(32) Alsfasser, R.; Powell, A. K.; Vahrenkamp, H. *Angew. Chem., Int. Ed. Engl.* **1990**, *29*, 898.
(33) (a) Luckay, R.; Cukrowski, I.; Mashishi, J.; Reibenspies, J. H.; Bond, A. H.; Rogers, R. D.; Hancock, R. D. *J. Chem. Soc., Dalton Trans.* **1997**, 901. (b) Rogers, R. D.; Bond, A. H.; Aguinaga, S. *J. Am. Chem. Soc.* **1992**, *114*, 2960. (c) Rogers, R. D.; Bond, A. H.; Aguinaga, S.; Reyes, A. *J. Am. Chem. Soc.* **1992**, *114*, 2967.
(34) Ōkawa, H.; Tokii, T.; Nonaka, Y.; Muto, Y.; Kida, S. *Bull. Chem. Soc. Jpn.* **1973**, *46*, 1462.
(35) Bosnich, B. *J. Am. Chem. Soc.* **1968**, *90*, 627.
(36) Downing, R. S.; Urbach, F. C. *J. Am. Chem. Soc.* **1969**, *91*, 5977.

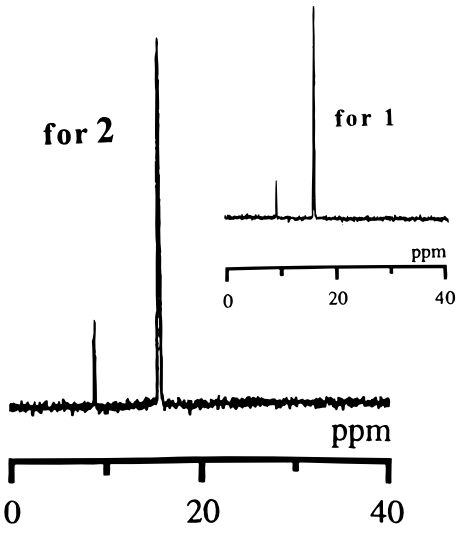

Figure 4. ^{31}P NMR spectrum for a DMSO solution containing 1×10^{-3} mol of **2** and 1×10^{-2} mol of TNP ([**2**]/[TNP] = 1/10). The insert shows the ^{31}P NMR spectrum with **1** under the same conditions.

Hydrolytic Activity toward TNP. The hydrolytic activity of the ZnPb complexes **1** and **2** toward tris(*p*-nitrophenyl) phosphate (TNP) has been examined by ^{31}P NMR spectroscopy in DMSO. A DMSO solution containing 1×10^{-3} mol of the complex (**1** or **2**) and 1×10^{-2} mol of TNP ([complex]/[TNP] = 1/10) was prepared, allowed to stand overnight, and subjected to ^{31}P NMR measurements. The results are given in Figure 4. The signal at −16.040 ppm is attributed to TNP and the signal at −9.179 ppm to BNP^- liberated from TNP.[16] The intensity ratio of the signals is $[TNP]/[BNP^-] \approx 9:1$ for both **1** and **2**, indicating a practically stoichiometric hydrolysis of TNP by these complexes. In parallel experiments, we confirmed that the corresponding $Ni^{II}Pb^{II}$ complex, $[NiPb(L)](ClO_4)_2 \cdot 2H_2O$, cannot hydrolyze TNP. Furthermore, the addition of $[Zn(salen)(H_2O)]$ and Pb^{2+} ion (1:1) could not hydrolyze TNP. These observations clearly indicate that the pair of Zn^{II} and Pb^{II} ions in close proximity plays an essential role in the hydrolysis of TNP.

The hydrolysis of TNP by **1** and **2** in DMSO was also followed by visible spectroscopy. An absorption band typical of *p*-nitrophenolate ion[37] appeared at 432 nm whose intensity increased with time and converged. The time courses of the absorbance at 432 nm at 25 °C are shown in Figure 5. It is seen that the hydrolysis by **1** takes about 30 min, whereas the hydrolysis by **2** is completed in 5 min. Evidently, **2** has a high activity but **1** has a low activity, demonstrating that the $Zn^{II}(OH)Pb^{II}$ core with a hydroxo group on the Zn^{II} is essential for the efficient hydrolysis of TNP to BNP^-. The activity of **1** may be explained by a partial dissociation of **1** into **2** ($[ZnPb(L)(H_2O)]^{2+} \rightleftharpoons [ZnPb(L)(OH)]^{+} + H^{+}$). This can also explain why the absorbance at 432 nm observed for the hydrolysis by **1** is weaker than that observed for the hydrolysis by **2**; the reaction solution with **1** is more acidic compared with that with **2** to supress the deprotonation of *p*-nitrophenolate liberated from TNP.

From the TNP hydrolysis by **2**, a BNP^--containing complex, $[ZnPb(L)(BNP)]ClO_4$ (**3**), has been isolated. For practical purposes, **3** is prepared in a good yield by the reaction between **2** and TNP in acetonitrile (method 1 in the Experimental Section) or by the reaction between **1** and TNP in acetonitrile in the presence of triethylamine (method 2). An ORTEP drawing

(37) Dede, L.; Rosenberg, A. *Ber. Deut. Chem. Ges.* **1934**, *67*, 147.

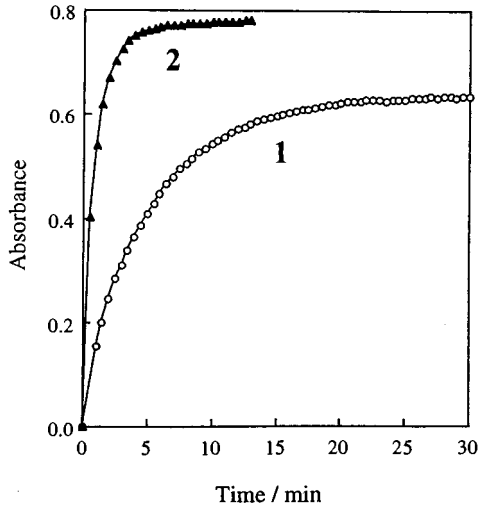

Figure 5. Time courses of the absorbance intensity at 432 nm in the TNP hydrolysis by **1** and **2**. Conditions were as follows: [complex] = 1×10^{-3} M; [TNP] = 3.3×10^{-5} M in DMSO (3 cm^3) at at 25 °C.

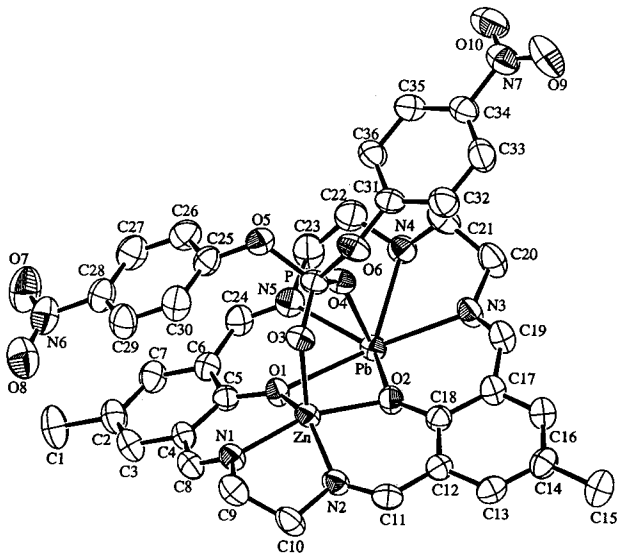

Figure 6. ORTEP view of the cation of **3** with the atom numbering scheme.

of the cation of **3** is given in Figure 6 together with the atom numbering scheme. The relevant bond distances and angles are given in Table 4.

The essential part of **3** consists of Zn^{II} and Pb^{II} ions, the macrocycle $(L)^{2-}$, and one BNP^- group; the perchlorate ion is free from coordination and captured in the lattice. The Zn resides at the "salen" site, and the Pb resides at the "saldien" site. The two metal ions are bridged by two phenolic oxygens O1 and O2 of the macrocycle $(L)^{2-}$ and the BNP^- group through its O3 and O4 oxygens in the intermetallic separation of 3.464(2) Å.

The geometry about the Zn is square pyramidal with N1, N2, O1, and O2 of the macrocycle on the basal plane and O3 of the BNP^- group at the apex. The Zn is displaced by 0.46 Å from the basal least-squares plane toward O3. The basal Zn−N and Zn−O bond distances are in the range 2.035(5)−2.054(7) Å. The axial Zn−O3 distance is 1.993(6) Å, which is shorter than the basal Zn−L bond distances.

The Pb at the "saldien" site has a six-coordinate geometry together with a bridging BNP^- oxygen. The geometry about the Pb is a pentagonal pyramid with O1, O2, N3, N4, and N5

Table 4. Relevant Bond Distances and Angles for **3**

Bond Distances (Å)			
Zn−O(1)	2.044(6)	Pb−O(1)	2.519(5)
Zn−O(2)	2.035(5)	Pb−O(2)	2.608(5)
Zn−O(3)	1.993(6)	Pb−O(4)	2.360(5)
Zn−N(1)	2.046(7)	Pb−N(3)	2.554(7)
Zn−N(2)	2.054(7)	Pb−N(4)	2.549(7)
P−O(3)	1.492(6)	Pb−N(5)	2.565(7)
P−O(4)	1.480(6)		
P−O(5)	1.592(6)		
P−O(6)	1.595(6)		
Bond Angles (deg)			
O(1)−Zn−O(2)	93.4(2)	O(1)−Pb−O(2)	70.8(2)
O(1)−Zn−O(3)	92.3(2)	O(1)−Pb−O(4)	76.3(2)
O(1)−Zn−N(1)	88.1(3)	O(1)−Pb−N(3)	138.3(2)
O(1)−Zn−N(2)	161.0(3)	O(1)−Pb−N(4)	135.0(2)
O(2)−Zn−O(3)	99.2(3)	O(1)−Pb−N(5)	71.7(2)
O(2)−Zn−N(1)	143.9(3)	O(2)−Pb−O(4)	75.5(2)
O(2)−Zn−N(2)	88.5(2)	O(2)−Pb−N(3)	70.5(2)
O(3)−Zn−N(1)	116.8(3)	O(2)−Pb−N(4)	133.8(2)
O(3)−Zn−N(2)	106.1(3)	O(2)−Pb−N(5)	138.6(2)
N(1)−Zn−N(2)	79.4(3)	O(4)−Pb−N(3)	79.8(2)
Pb−O(1)−Zn	98.3(2)	O(4)−Pb−N(4)	76.4(2)
Pb−O(2)−Zn	97.5(2)	O(4)−Pb−N(5)	79.4(2)
O(3)−P−O(4)	119.5(3)	N(3)−Pb−N(4)	68.9(2)
O(3)−P−O(5)	109.9(3)	N(3)−Pb−N(5)	135.8(2)
O(3)−P−O(6)	105.5(3)	N(4)−Pb−N(5)	68.5(2)
O(4)−P−O(5)	109.5(3)	Zn−O(3)−P	123.6(3)
O(4)−P−O(6)	110.6(3)	Pb−O(4)−P	138.8(3)
O(5)−P−O(6)	99.9(3)		

of the "saldien" site on the base and O4 of the BNP^- group at the axial position. The core geometry of **3** resembles that of the half-unit of dimeric **2′**. The sum of the bond angles O1−Pb−O2, O2−Pb−N3, N3−Pb−N4, N4−Pb−N5, and O1−Pb−N5 is 350.4°. The in-plane Pb-to-L bond distances range from 2.519(5) to 2.608(5) Å. The Pb−O3 bond distance is short (2.360(5) Å). The Pb is displaced by 0.52 Å from the basal least-squares plane toward the open space. Thus, the Pb assumes a similar "umbrella-like" shape.

In the BNP^- bridge, the P−O3 and P−O4 bond distances (1.492(6) and 1.480(6) Å, respectively) are significantly shorter than the P−O5 and P−O6 bond distances (1.592(6) and 1.595(6) Å, respectively). The O3−P−O4 bond angle is large (119.5(3)°). Instead, the O5−P−O6 bond angle is small (99.9(3)°). The remaining O−P−O bond angles fall in the range 105.5(3)−110.6(3)° that is common for tetrahedral phosphorus. The geometrical feature of the BNP^- in **3** is similar to that found in other bimetallic complexes bridged by phosphate ester ligands.[15,16]

Chart 2 Proposed Mechanism for TNP Hydrolysis by **2**

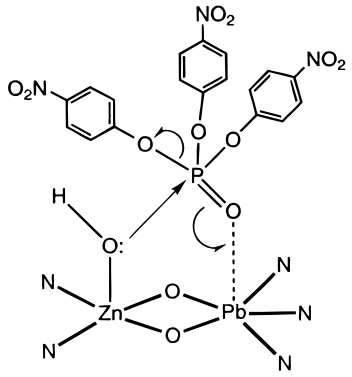

On the basis of the above studies, a mechanistic scheme for the TNP hydrolysis by **2** is proposed (Chart 2). A TNP molecule is bound to the Pb center through its oxygen, and the hydroxide on the adjacent Zn ion attacks the phosphorus nucleus of TNP, leading to the formation of the BNP^- complex **3**. Thus, the present study illustrates a functional model of the heterobimetallic phosphatases, and **3** can be regarded as the intermediate in biological hydrolysis of phosphate triesters. We have noticed that the [TNP]/[BNP^-] ratio in the ^{31}P NMR study using **2** (Figure 4) gradually decreases from 9/1 (stoichiometric) to ~8/2 after 1 week. This fact means that the BNP^- bridge is partially dissociated and affords **1** together with water supplied from the atmosphere. A catalytic cycle for the TNP hydrolysis may be possible by the choice of an appropriate $Zn^{II}M^{II}$ pair.

Acknowledgment. This work was supported by a Grant-in-Aid for Scientific Research (09440231) from the Ministry of Education, Science and Culture, Japan. We would like to thank Daiwa Anglo of the Japanese Foundation and the British Council for their support. Thanks are also due to Associate Professor Kazuhiro Takahashi and Dr. Masaaki Ohba of Kyushu University for valuable discussions.

Supporting Information Available: X-ray crystallographic files, in CIF format, for **1**−**3** and **1′**−**3′** are available on the Internet only. Access information is given on any current masthead page.

IC9804869